

## Formation and Structure of a Dense Octahedral Glass

M. Guthrie,<sup>1,2,\*</sup> C. A. Tulk,<sup>1</sup> C. J. Benmore,<sup>2</sup> J. Xu,<sup>3</sup> J. L. Yarger,<sup>4</sup> D. D. Klug,<sup>5</sup> J. S. Tse,<sup>5</sup> H.-k. Mao,<sup>3</sup> and R. J. Hemley<sup>3</sup>

<sup>1</sup>*Oak Ridge National Laboratory, Oak Ridge, Tennessee 37831 USA*

<sup>2</sup>*Argonne National Laboratory, Argonne, Illinois 60439 USA*

<sup>3</sup>*Carnegie Institution of Washington, 5251 Broadbranch Road, N.W., Washington, D.C. 20015 USA*

<sup>4</sup>*University of Wyoming, Laramie, Wyoming 82071 USA*

<sup>5</sup>*National Research Council of Canada, Ottawa, Ontario, K1A 0R6 Canada*

(Received 5 March 2004; published 10 September 2004)

We have performed *in situ* x-ray and neutron-diffraction measurements, and molecular dynamics simulations, of GeO<sub>2</sub>, an archetypal network-forming glass under pressure. Below 5 GPa, additional atoms encroaching on the first tetrahedral shell are seen to be a precursor of local coordination change. Between 6 and 10 GPa, we observe structures with a constant average coordination of  $\sim 5$ , indicating a new metastable, intermediate form of the glass. At 15 GPa, the structure of a fully octahedral glass has been measured. This structure is not retained upon decompression and, therefore, must be studied *in situ*.

DOI: 10.1103/PhysRevLett.93.115502

PACS numbers: 61.43.Fs, 61.10.-i, 61.12.-q

The structures of glasses and liquids at very high-pressure have generally not been studied with diffraction techniques. This is despite strong indications that, as in crystalline materials, their structural polymorphism may be rich [1,2]. Perhaps the most fundamentally important of these are the network-forming, tetrahedral-oxide glasses [3]. At high pressures, where optical and x-ray absorption spectroscopy (XAS) are believed to show a transition to a dense locally octahedral structure [4,5], the current understanding of the structure is severely limited. This has led to vigorous debate over the continuous *versus* discontinuous nature of the transformation, [2,6] the concurrent changes in intermediate-range order (IRO), which are unknown [4–6], and more general concepts of polyamorphism in glasses.

At ambient pressure classic network-forming glasses such as GeO<sub>2</sub> and SiO<sub>2</sub> exhibit both well-defined short-range order (SRO) and IRO [1,3,7]. Predensified samples (pressurized and recovered) display no change in local cation coordination [8,9]. While *in situ* diffraction measurements of these glasses are severely limited, XAS studies have shown a gradual increase in the covalent bond length in GeO<sub>2</sub> from 6 to 10 GPa, which attains a value close to that of the octahedrally coordinated crystalline phase (rutile) [4]. SiO<sub>2</sub> exhibits similar behavior, but at higher pressures [5]. As a result, a “first-order” amorphous-amorphous transition has been postulated [4,10,11]. Conversely, some vibrational spectroscopy studies claim the same transformations are continuous [6]. Fundamental questions regarding the compaction process itself and the details of the SRO and connectivity of the ultimate octahedral form remain unknown [12].

We report *in situ* x-ray measurements of the structure of glassy GeO<sub>2</sub> to 15 GPa, with complementary *in situ* neutron measurements up to 5 GPa and molecular dynamics (MD) studies of both the tetrahedral and octahedral form.

The neutron structure-factor data were collected on the GLAD instrument at the Intense Pulsed Neutron Source (IPNS) at Argonne National Laboratory (ANL). [13]. X-ray data were collected at the Sector 11 ID-C diffractometer at the Advanced Photon Source (APS) (also at ANL), using a high-energy (115 keV) monochromatic beam. Both samples were prepared by techniques described elsewhere [9]. The x-ray data more strongly represent the Ge-Ge and Ge-O correlations, while the neutron data are more heavily weighted toward O-O correlations [14].

For the neutron measurements, a V3 Paris-Edinburgh press [15] with TiZr null-scattering gaskets and specialized collimation was used. This successfully reduced the Bragg scattering from the anvils to <1% of the total diffracted signal. Experimental pressures were estimated using separately measured pressure-load curves for the Paris-Edinburgh press and, thus, have a limited accuracy estimated to be  $\pm 1$  GPa.

The x-ray samples had a volume of 1.1 mm<sup>3</sup> and were loaded as powders, without a pressure medium, into a novel large-volume moissanite anvil cell [16]. The effects of pressure gradients were minimized by using a beam significantly smaller than the diameter of the anvil tip. Pressures were measured using a ruby-fluorescence technique [17], and are accurate to  $+/- 0.2$  GPa. A separate measurement of GeO<sub>2</sub> only was also made. The difference between this “freestanding” sample and that measured with the sample inside the cell (with no load), gave the ambient-pressure background due to the cell itself. Changes in background with pressure were found to be dominated by geometrical changes in the cell. These were readily modeled by the addition of a single, broad Gaussian feature to the high-pressure backgrounds. Subsequent Fourier transformations of this *additive* background feature, demonstrate that it does not affect determination of physical features greater than 1.0 Å. Other

corrections were applied using the ISOMER-X [18] software package. Absorption and multiple scattering effects were assumed to be negligible at these high energies.

In order to provide additional insight into the experimental results, a MD study with a constant pressure ( $NpH$ ) ensemble in the DLPOLY code [19] was also performed on glassy  $\text{GeO}_2$  [20]. For the simulations, amorphous  $\text{GeO}_2$  was prepared by heating the cristobalite form with 400  $\text{GeO}_2$  to 7000 K and then cooling stepwise to 300 K. Another sample consisting of 2000  $\text{GeO}_2$  was prepared starting from the reverse Monte Carlo fit to the experimental structure factors followed by relaxation with MD to an amorphous sample. Both samples gave nearly identical radial distribution functions.

The most prominent signature of IRO is a first sharp diffraction peak (FSDP) [3] in the structure factor. The position of this peak,  $Q_p$  is inversely related to periodicities in the real-space structure. In addition, its height reflects the extent of these periodicities and the packing of structural elements [21]. Thus densification is observed to both reduce its height while increasing its position [22,23]. It has been argued that the IRO (in  $\text{GeO}_2$ ,  $\text{SiO}_2$ , and the chalcogenide network glasses), is associated with cages enclosing open regions of the network [24]. A recent diffraction study of predensified  $\text{GeO}_2$  glass at ambient pressure [9] indicated significant reduction of this network connectivity upon compaction. However, Hemley *et al.* have demonstrated the importance of studying such changes *in situ* [25].

Our neutron and x-ray diffraction measurements on glassy  $\text{GeO}_2$  to 6 GPa both reveal distinct trends in the FSDP. The total neutron structure factors  $S_n(Q)$  [Fig. 1(b)] show a dramatic, systematic decrease of peak height with pressure and a corresponding increase in height of the second peak. In contrast, equivalent x-ray

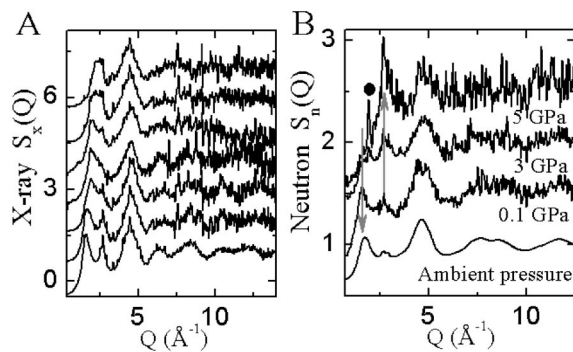


FIG. 1. (a) Shows x-ray  $S(Q)$  at 0, 3, 5, 6, 7, 10, and 15 GPa (bottom to top). (b) Shows equivalent neutron  $S(Q)$  data to 5 GPa, with ambient-pressure data from [9]. A filter was applied to the neutron data excluding sharp features more than 3 standard deviations above neighboring data points. The weak crystalline contamination, indicated by ●, present in the neutron measurements, was identified as  $\sim 2\text{--}3\%$   $\alpha$ -phase  $\text{GeO}_2$ .

structure factors  $S_x(Q)$  in Fig. 1(a) show a gradual shift of the FSDP to higher  $Q$  where it merges with the second peak. This implies that the breakdown of IRO upon compaction of the tetrahedral network in  $\text{GeO}_2$  glass is mainly associated with changes in the oxygen correlations, which are probed more strongly by neutron diffraction. These data indicate that, prior to coordination change, the pressure-induced changes in  $\text{GeO}_2$  probably result from a decrease in size and eventual collapse of the ambient-pressure cage structures as the network is compacted.

Subsequently, the  $S_x(Q)$  data were Fourier transformed to give total-distribution functions  $T(r)$  using the relation [26]

$$S_x(Q) = \int_0^\infty Q[T_x(r) - 4\pi\rho r] \sin(Qr) dr.$$

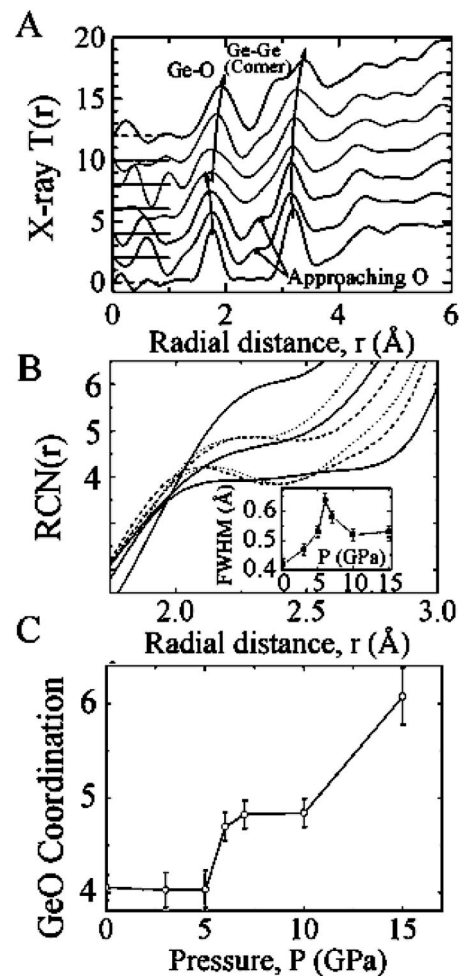


FIG. 2. (a) X-ray  $T(r)$  data with densities in  $\text{atoms}/\text{\AA}^3$  of 0.064, 0.070, 0.077, 0.081, 0.084, 0.092, and 0.100 (extrapolated) [26]. (b) Corresponding running-coordination numbers (RCN). The inset shows the full width at half maximum of the first  $T(r)$  peak versus pressure. (c) The coordination number from the measured inflection point, or average oscillation, in the RCN.

These functions, shown in Fig. 2(a), depict total average density (weighted by the atomic form factors of the individual atoms Ge and O) as a function of radial distance  $r$ . At 0 GPa, the  $T(r)$  demonstrates the characteristic features of a tetrahedral-network structure [1,8,9]. The strong peaks at 1.76(4) Å and 3.20(4) Å arise, respectively, from the covalent Ge—O bond and the intertetrahedral Ge-Ge correlations between corner-shared tetrahedra. The peak at 4.51(4) Å is attributable to the Ge-O correlation between next-nearest-neighbor tetrahedra.

Below 6 GPa, in both experiment and simulation, we observe a reduction in Ge—O bond length and concurrent peak broadening. We also observe a new peak at  $\sim 2.5$  Å at 3 and 5 GPa that is not observed in predensified GeO<sub>2</sub> samples [8,9], Fig. 2(a). This short distance and the relative weakness of the oxygen partial in the x-ray data suggest the peak is unlikely to arise from intratetrahedral O-O correlations. Likewise, Ge-Ge correlations are discounted: such a short distance would imply edge sharing between tetrahedral units, thus violating stoichiometric constraints. Also, such a dramatic structural change would certainly result in drastic changes in the Raman spectrum that are not observed [11]. Thus, we attribute the 2.5 Å peak to a new Ge-O correlation, and note that it may be related to a slight increase in intensity across a similar  $Q$ -range observed in densified SiO<sub>2</sub> [23]. The appearance of this peak is supported by an increased Ge-O intensity in this region observed during our MD simulations in this pressure range.

The Ge-O coordination number for these data are shown in Figs. 2(b) and 2(c). Below 6 GPa a tetrahedral local unit is observed, although the increasing peak width [see Fig. 2(b), inset] shows substantial distortion. By 6 GPa, the coordination number increases to 4.8 (2). Subsequently, at both 7 and 10 GPa, distinct plateaus are seen in the running-coordination numbers (RCN) at just below five.

A narrowing Ge-O peak width, concurrent with a constant coordination number of nearly five, is consistent with the formation of pentahedra: first as highly-distorted tetrahedra with nonbonded oxygen atoms forced into the close proximity. Pentahedrally coordinated cations have been previously reported, e.g., in simulations of SiO<sub>2</sub> [27], experiments on CaSiO<sub>5</sub> [28], and aluminosilicate melts with <sup>29</sup>Si stable during transformation processes [29,30]. As the coordination number measured here is a bulk average, a value of five can also be accounted for by an equal mixture of fourfold and sixfold units. Coexistence of both polyhedra was proposed in the original XAS study to account for the observed bond length behavior [4], however, in this case a continuous increase of coordination number is expected throughout the transition. The data are however consistent with the MD simulations showing that Ge atoms become coordi-

nated with five oxygen atoms during the transformation. The additional oxygen correlations are probably the result of encroachment of the new Ge-O correlation, first observed at 3 GPa, upon the first coordination shell. Thus, the densification below 6 GPa is a necessary precursor to the subsequent transition.

At 15 GPa, the local coordination has increased to six. This implies further structural change between 10 and 15 GPa, specifically, additional oxygen must enter the first coordination shell.

The octahedral pattern is characterized by several distinct and pronounced peaks [Fig. 3(a)]. The Ge-O peak in the octahedral glass is centered on 1.91(2) Å. This bond length is significantly larger than the XAS value of 1.83 Å [4], but is consistent with that found within planes of edge-shared octahedra in the crystalline rutile phase of 1.87 Å (at 16 GPa) [31]. A characteristic feature of the

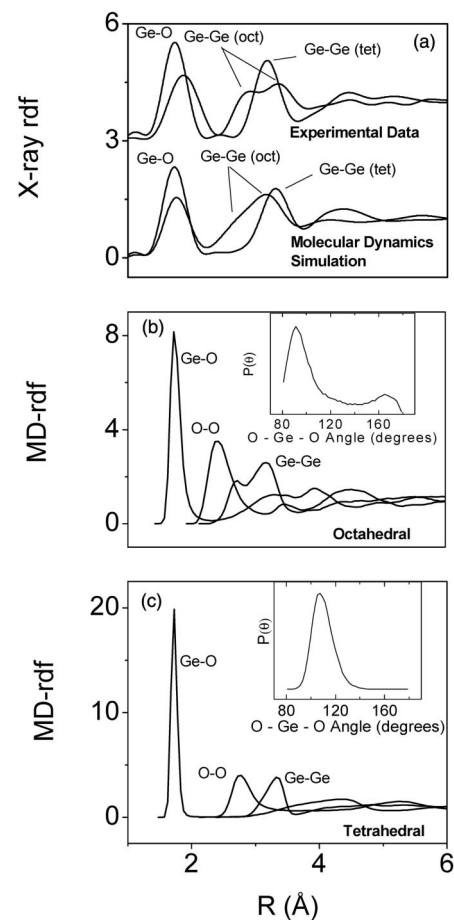


FIG. 3. . A direct comparison of the measured ((a) upper) and MD simulated ((a) lower) x-ray weighted radial distribution function data. The MD simulated partial radial distribution functions are given in (b) and (c) (plotted with an equal scaling). The MD calculations were done at densities of 0.064 atoms/Å<sup>3</sup> for the tetrahedral form, and 0.132 atoms/Å<sup>3</sup> for the octahedral form.

octahedral glass is the strong peak, centered on 2.83(2) Å at the expected location for edge-shared Ge-Ge correlations, required to maintain stoichiometry.

Resulting partial radial distribution functions (RDFs) from the MD analysis are shown in Figs. 3(b) and 3(c). The MD simulations indeed show that GeO<sub>2</sub> can be densified to a fully six-coordinated structure albeit at higher pressures than in the experiment due to kinetic effects. In a sample pressurized to 20 GPa, we found that after annealing at 1000 K for 110 ps, the Ge-O coordination increases from 5.3 to 5.6 with a cutoff of 2.4 Å. The MD revealed a full six coordination when the density was increased to 0.132 atom/Å. An analysis of the O—Ge—O bond angles of an overpressurized sample was carried out [insets, Fig. 3(b) and 3(c)] and indicates that the local structure about Ge atoms is close to that of an octahedron with a maximum in the O-Ge-O angle distribution near 90° and a weak maximum near 165°. For a perfect octahedron these angles should be 90° and 180°, respectively. At all pressures above ~6 GPa, there are two distinct peaks in the Ge-Ge partial RDFs in the 2.5–3.5 Å region. This is consistent with the presence of edge-shared and corner-shared octahedra that are seen from inspection of the structure in the MD calculations. Of the neighboring Ge, approximately 20% involve edge-shared and 80% involve corner-shared polyhedra. We see no evidence of the short-range Ge-Ge correlations that would indicate *face*-shared octahedra.

Using these novel techniques, we have performed detailed structural characterization of a high-pressure glass. These new methods facilitate the detailed study of structural transformations in amorphous solids and, in the case of GeO<sub>2</sub>, we observe significant changes in IRO and stable intermediately-coordinated structures. Finally, we have obtained diffraction measurements of a dense octahedral glass that are supported by MD simulations thus providing an opportunity for determination of its extended structure.

The SNS is managed by UT-Battelle, LLC under Contract No. DE-AC05-00OR22725 for the U.S. DOE, and the U.S. DOE Contract No. W31109ENG 38 was used for measurements at IPNS and APS, ANL. The work at Carnegie was supported by the NSF and DOE (CDAC). We also acknowledge the support of Y. Ren on BESSRC and the staff at Sectors 11 and 13. We also wish to thank J. Neuefeind, D.L. Price, S. Sampath, J. Siewenie and J. Burley.

---

\*Present Address: CSEC, School of Physics, University of Edinburgh, Edinburgh, United Kingdom, EH9 3JZ.

- [1] A. C. Wright *et al.*, *J. Non-Cryst. Solids* **49**, 63 (1982).  
 [2] P. F. McMillan, in *High Pressure Phenomena*, edited by R. J. Hemley and G. L. Chiarotti (IOS Press, Amsterdam, 2002).

- [3] A. C. Wright, *J. Non-Cryst. Solids* **179**, 84 (1994).  
 [4] J. P. Itié *et al.*, *Phys. Rev. Lett.* **63**, 398 (1989).  
 [5] C. Meade, R. J. Hemley, and H.-k. Mao, *Phys. Rev. Lett.* **69**, 1387 (1992).  
 [6] M. Grimsditch, *Phys. Rev. Lett.* **52**, 2379 (1984); Q. Williams and R. Jeanloz, *Science* **239**, 902 (1988).  
 [7] D. L. Price, M.-L. Saboungi, and A. C. Barnes, *Phys. Rev. Lett.* **81**, 3207 (1998).  
 [8] C. E. Stone *et al.*, *J. Non-Cryst. Solids* **293**, 769 (2001).  
 [9] S. Sampath *et al.*, *Phys. Rev. Lett.* **90**, 115502 (2003).  
 [10] O. Ohtaka *et al.*, *J. Phys. Condens. Matter* **14**, 10521 (2002).  
 [11] D. J. Durben and G. H. Wolf, *Phys. Rev. B* **43**, 2355 (1991).  
 [12] R. J. Hemley, J. Badro, and D. M. Teter, in *Physics Meets Mineralogy— Condensed Matter Physics in Geosciences*, edited by H. Aoki, Y. Syono, R. J. Hemley (Cambridge University Press, Cambridge, 2000), p. 173.  
 [13] R. K. Crawford *et al.*, *Inst. Phys. Conf. Ser.* **97**, 427 (1989).  
 [14] For the x-ray case, the relative percentages of the partials in the measured  $S(Q)$  at  $Q = 0 \text{ \AA}^{-1}$  are: 45% Ge-Ge, 44% Ge-O, and only 11% for O-O correlations. For  $Q > 0 \text{ \AA}^{-1}$ , the O-O contribution is reduced still further, dropping to less than 6% by  $5 \text{ \AA}^{-1}$ . For the neutron case, the weights are  $Q$  independent and are: 17% Ge-Ge, 49% Ge-O, and 34% O-O.  
 [15] J. M. Besson *et al.*, *Physica B (Amsterdam)* **180**, 907 (1993).  
 [16] J. Xu, H.-k. Mao, *Science* **290**, 783 (2000).  
 [17] H.-k. Mao, J. Xu, and P. M. Bell, *J. Geophys. Res.* **91**, 4673 (1986).  
 [18] J. Urquidi, C. J. Benmore, J. Neuefeind, and B. Tomberli, *J. Appl. Crystallogr.* **36**, 368 (2003).  
 [19] W. Smith, M. Leslie and T. R. Forester, *The DL\_POLY\_2 User Manual*, Version 2.11 (CCLRC, Daresbury Laboratory, Daresbury, England, WA4 4AD 2003).  
 [20] T. Tsuchiya, T. Yamanaka, and M. Matsui, *Phys. Chem. Miner.* **25**, 94 (1998).  
 [21] S. C. Moss and D. L. Price, in *Physics of Disordered Materials*, edited by D. Adler, H. Fritzsche, and S. Ovshinky (Plenum Press, New York, 1985), Vol. 1.  
 [22] S. R. Elliott, *Phys. Rev. Lett.* **67**, 711 (1991).  
 [23] S. Susman *et al.*, *Phys. Rev. B* **43**, 1194 (1991).  
 [24] A. C. Wright, R. N. Sinclair, and A. J. Leadbetter, *J. Non-Cryst. Solids* **71**, 295 (1985).  
 [25] R. J. Hemley, C. Meade, H.-k. Mao, *Phys. Rev. Lett.* **79**, 1420 (1997).  
 [26] O. B. Tsiok, V. V. Brazhkin, A. G. Lyapin, and L. G. Khvostantsev, *Phys. Rev. Lett.* **80**, 999 (1998).  
 [27] J. Badro *et al.*, *Phys. Rev. B* **56**, 5797 (1997).  
 [28] R. Angel, N. L. Ross, F. Seifert, and T. F. Fliervoet, *Nature (London)* **384**, 441 (1996).  
 [29] *Reviews in Mineralogy: Structure, Dynamics and Properties of Silicate Melts*, edited by J. F. Stebbins, P. F. McMillan, and D. B. Dingwell (Mineralogical Society of America, Washington, D.C., 1995).  
 [30] M. C. Warren, S. A. T. Redfern, and R. Angel, *Phys. Rev. B* **59**, 9149 (1999).  
 [31] J. Haines, J. M. Léger, C. Chateau, and A. S. Pereira, *Phys. Chem. Miner.* **27**, 575 (2000).